Cancer Immunology, Immunotherapy (2025) 74:159
https://doi.org/10.1007/s00262-025-04015-1

RESEARCH

Single-cell RNA sequencing reveals an IL1R2+Treg subset driving immunosuppressive microenvironment in HNSCC

Haiyan Guo[1] · Chun Liu[2] · Kun Wu[3] · Yan Li[4] · Zhen Zhang[1,2,5] · Fuxiang Chen[1,6]

Received: 10 February 2025 / Accepted: 5 March 2025 / Published online: 25 March 2025

Abstract

Regulatory T cells (Tregs) play an immunosuppressive role in tumor microenvironment (TME) in various of cancer types. However, how different Treg subsets influence and effect on head and neck squamous cell carcinoma (HNSCC) remain unclear. Here, using single-cell RNA sequencing (scRNA-seq), we identified an IL1R2+Treg subset which promoted the progression of HNSCC. Via tissue microassay (TMA) and enzyme-linked immunosorbent assay (ELISA), we verified the clinical diagnostic value of the IL1R2+Treg and soluble IL1R2 (sIL1R2). In addition, we constructed tumor-bearing mouse models to explore the antitumor effects of combined targeting IL1R2 and CTLA4. For mechanism, we found IL-1β promoted the expression of IL1R2 and CTLA4 in Tregs, and upregulated CTLA4 though NR4A1 translocation. These results revealed that IL1R2+Treg and serum IL1R2 level had potential diagnostic and prognostic value of HNSCC and combined targeting of IL1R2 and CTLA4 might be an effective strategy to inhibit tumor progression.

Keywords Head and neck squamous cell carcinoma · Regulatory T cell · Interleukin-1 receptor 2 · Cytotoxic T lymphocyte-associated antigen-4

Introduction

Tregs are a subgroup of CD4+T cells, that are characterized by the expression of forkhead box protein 3 (Foxp3) and CD25. In the tumor microenvironment (TME), regulatory T cells (Tregs) play an immunosuppressive role, severely weakening the antitumor-specific immune response [1]. Tregs exert immunosuppressive effects by secreting inhibitory cytokines, upregulating inhibitory receptors, and depriving the local TME of IL-2 through high expression of CD25 [2–4]. These data indicate that Tregs promote the formation of immunosuppressive TME via multiple mechanisms in HNSCC and that the inhibition of Tregs may enhance the immunotherapy response.

Haiyan Guo and Chun Liu have contributed equally to this work.

✉ Zhen Zhang
zhangzhen1007@sjtu.edu.cn

✉ Fuxiang Chen
chenfx@sjtu.edu.cn

Haiyan Guo
sxguohaiyan@126.com

Chun Liu
joelau3738@sjtu.edu.cn

Kun Wu
wukun1302@csu.edu.cn

Yan Li
liyan1106369@163.com

[1] Department of Clinical Immunology, Shanghai Ninth People's Hospital, Shanghai Jiao Tong University School of Medicine, 639 Zhizaoju Road, Shanghai 200011, China

[2] Department of Oral and Maxillofacial-Head and Neck Oncology, Shanghai Ninth People's Hospital, Shanghai Jiao Tong University School of Medicine, Shanghai, China

[3] Department of Oral and Maxillofacial Surgery, Second Xiangya Hospital of Central South University, Changsha, China

[4] Precision Research Center for Refractory Diseases, Shanghai General Hospital, Shanghai Jiao Tong University School of Medicine, Shanghai, China

[5] Diagnosis and Treatment Innovation Center for Cancer, Institute of Translational Medicine, Shanghai Jiao Tong University, Shanghai, China

[6] Faculty of Medical Laboratory Science, College of Health Science and Technology, Shanghai Jiao Tong University School of Medicine, Shanghai, China

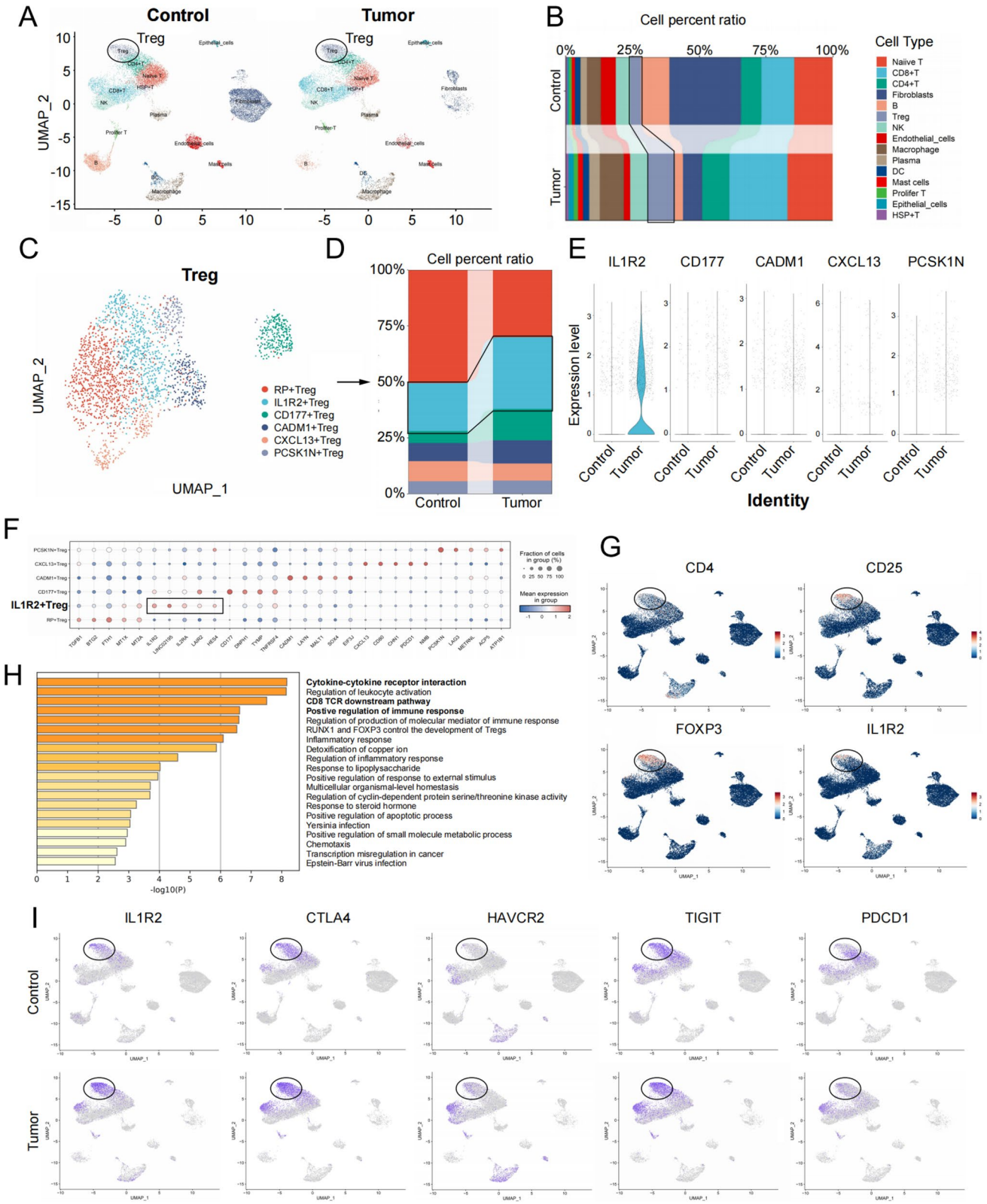
A
Control
Tumor
Treg
UMAP_2
B
Cell percent ratio
Control
Tumor
Cell Type
Naiive T
CD8+T
CD4+T
Fibroblasts
B
Treg
NK
Endothelial_cells
Macrophage
Plasma
DC
Mast cells
Prolifer T
Epithelial_cells
HSP+T
C
Treg
UMAP_1
RP+Treg
IL1R2+Treg
CD177+Treg
CADM1+Treg
CXCL13+Treg
PCSK1N+Treg
D
Cell percent ratio
Control
Tumor
E
IL1R2
CD177
CADM1
CXCL13
PCSK1N
Expression level
Identity
F
IL1R2+Treg
Fraction of cells in group (%)
Mean expression in group
G
CD4
CD25
FOXP3
IL1R2
H
Cytokine-cytokine receptor interaction
Regulation of leukocyte activation
CD8 TCR downstream pathway
Postive regulation of immune response
Regulation of production of molecular mediator of immune response
RUNX1 and FOXP3 control the development of Tregs
Inflammatory response
Detoxification of copper ion
Regulation of inflammatory response
Response to lipoplysaccharide
Positive regulation of response to external stimulus
Multicellular organismal-level homestasis
Regulation of cyclin-dependent protein serine/threonine kinase activity
Response to steroid hormone
Positive regulation of apoptotic process
Yersinia infection
Positive regulation of small molecule metabolic process
Chemotaxis
Transcription misregulation in cancer
Epstein-Barr virus infection
-log10(P)
I
IL1R2
CTLA4
HAVCR2
TIGIT
PDCD1
Control
Tumor

◂**Fig. 1** Tumor specific IL1R2+Treg in HNSCC tissues. **A** Combined UMAP plot showing clusters of cells in control (adjacent normal tissues, left panel) and tumor tissues (right panel) from 5 HNSCC patients. **B** Percentages of cell types, related to Fig. 1A. **C** UMAP plot of 6 Treg subsets from total Tregs. **D** Bar plots showing the proportions of Treg subsets in adjacent normal tissues and tumor tissues. **E** Expression level of marker genes in adjacent normal tissues and tumor tissues. **F** Bubble charts showing the identified marker of Treg subsets. **G** UMAP plots of all cells colored according to the expression level of CD4, CD25, FOXP3 and IL1R2. **H** GO analysis showing the function of IL1R2+Treg. **I** UMAP plots of all cells colored according to the expression of IL1R2, CTLA4, HAVCR2, TIGIT and PDCD1. Control, adjacent normal tissues; Tumor, tumor tissues

IL1R2, acts as a decoy receptor, can competitively bind to the common ligand IL-1α or IL-1β, especially IL-1β, through extracellular domains similar to those of IL1R1 [5, 6]. IL1R2 is highly expressed in a variety of cell types, including monocytes, macrophages, neutrophils, and B cells [7, 8]. IL1R2 can play an important role in tumorigenesis, invasion and metastasis via the regulation of inflammation and immunity [9, 10]. In addition, IL1R2 acts as a transcription co-factor to regulate the expression of the IL-6 and vascular endothelial growth factor A (VEGF-A) genes [11]. Also, IL1R2 promotes the proliferation of clear cell renal cell carcinoma cells by regulating the JAK2/STAT3 signaling pathway, and these functions are regulated by the intracellular domain of IL1R2 [12]. Thus, IL1R2 not only participates in the regulation of the inflammatory response by competing with IL1R1 and binding to IL-1 but also has biological activity as a transcriptional co-factor.

In this study, we identified an IL1R2+Treg subset, which was positively correlated with tumor progression in HNSCC and both IL1R2+Treg and soluble IL1R2 level in serum showed diagnostic and therapeutic value in HNSCC. What's more, we found IL-1β promoted the expression of IL1R2 and further upregulated CTLA4 through NR4A1 in Tregs. In vivo experiments also indicated that combined using si-il1r2 and anti-CTLA4 could reverse immunosuppressive TME, which might be an effective strategy to inhibit HNSCC progression.

Methods

Patients and sample collection

Five pairs of tumor tissue and adjacent tissue for scRNA-seq analysis were obtained from patients with HNSCC treated at the Ninth People's Hospital Affiliated to Shanghai Jiao Tong University School of Medicine from March 2019 to June 2019. The samples for multiplex immunohistochemical staining (mIHC) were obtained from patients of HNSCC who underwent surgery in 2023. The tissue microarray (TMA) for IL1R2+Treg infiltration analysis was obtained from HNSCC patients who underwent surgery from 2014 to 2024.

Single-cell RNA sequencing (scRNA-seq)

Tissue samples were washed with saline and immediately immersed in Miltenyi Tissue preservation Solution (No. 130–100-008). The tissue samples were cut into small pieces of about 0.5 mm^3 and digested into a single-cell suspension. Red Blood Cell Lysis Buffer (MACS, 130–094-183) was added to the cell precipitate for 5 min. After centrifugation, the cells were washed and re-suspended with RPMI-1640. The cDNA library was constructed using the 10 × Genomics Chromium Next GEM Single Cell 3'Reagent Kits v3.1 kit (No. 1000268). Sequencing was performed on Illumina Nova 6000 PE150 platform.

Multiplex immunohistochemical (mIHC) staining

The permeabilization for tissue sections was conducted with 0.5% TritonX-100 in PBST. Fc-blocking was conducted with 10% goat serum at room temperature. Primary antibody (Round 1: IL1R2 antibody, sigma, 1:200; Round 2: CD4 antibody, CST, 1:200; Round 3: FOXP3 antibody, CST, 1:200; Round 4: IL-1β antibody, Proteintech, 1:200) was added and incubated at 4℃ overnight. Secondary antibody was incubated at room temperature for 20 min. Fluorescence-conjugated HRP (MCE) was added and incubated at room temperature for 20 min. DAPI (Beyotime) was dripped onto the slices and incubated in a shaker at room temperature for 20 min. The slices were added with an anti-fluorescence quencher and sealed with a cover glass. Take pictures with confocal microscope.

Enzyme-linked immunosorbent assay (ELISA)

All steps are performed according to the instructions of IL1R2 ELISA Kit (FineTest, #EH0187). Set standard holes, blank holes and sample holes, and add 100 µl sample to each hole. The sample plates were incubated at 37 °C for 90 min. After cleaning, 100 µl biotin-antibody working solution was added to each well and incubated at 37℃ for 60 min. After cleaning, 100 µl HRP-Streptavidin working solution was added to each well and incubated at 37℃ for 30 min. After washing, 100 µl TMB solution was added to each well, incubated at 37℃, then 50 µl reaction

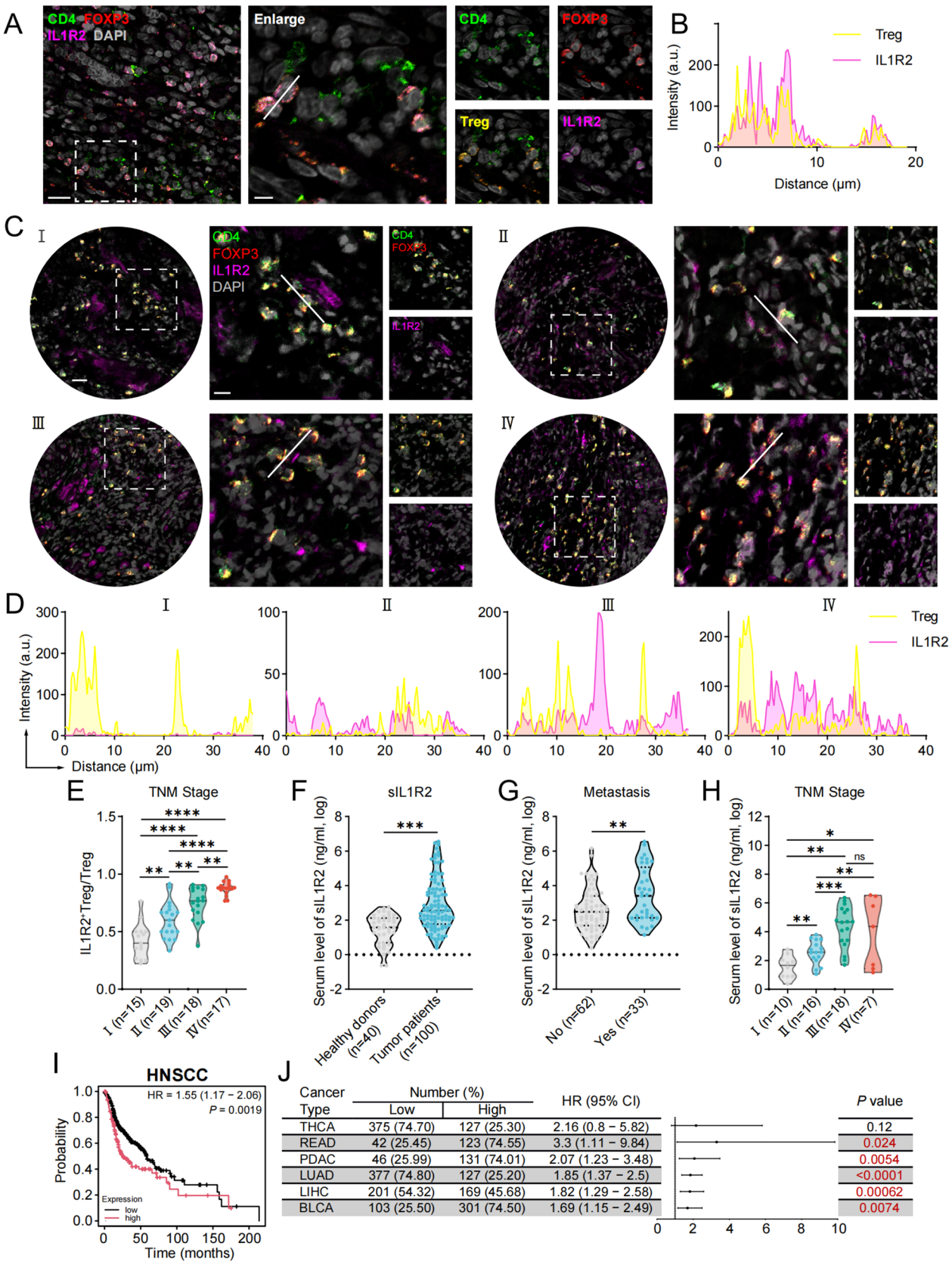
A
CD4 FOXP3
IL1R2 DAPI
Enlarge
CD4
FOXP3
Treg
IL1R2
B
Treg
IL1R2
Intensity (a.u.)
Distance (μm)
C
I
II
III
IV
CD4
FOXP3
IL1R2
DAPI
D
Intensity (a.u.)
Distance (μm)
Treg
IL1R2
E
TNM Stage
IL1R2+Treg/Treg
I (n=15)
II (n=19)
III (n=18)
IV (n=17)
F
sIL1R2
Serum level of sIL1R2 (ng/ml, log)
Healthy donors (n=40)
Tumor patients (n=100)
G
Metastasis
Serum level of sIL1R2 (ng/ml, log)
No (n=62)
Yes (n=33)
H
TNM Stage
Serum level of sIL1R2 (ng/ml, log)
I (n=10)
II (n=16)
III (n=18)
IV (n=7)
ns
I
HNSCC
HR = 1.55 (1.17 − 2.06)
P = 0.0019
Probability
Expression
low
high
Time (months)
J
Cancer Type
Number (%)
Low
High
HR (95% CI)
P value
THCA 375 (74.70) 127 (25.30) 2.16 (0.8 − 5.82) 0.12
READ 42 (25.45) 123 (74.55) 3.3 (1.11 − 9.84) 0.024
PDAC 46 (25.99) 131 (74.01) 2.07 (1.23 − 3.48) 0.0054
LUAD 377 (74.80) 127 (25.20) 1.85 (1.37 − 2.5) <0.0001
LIHC 201 (54.32) 169 (45.68) 1.82 (1.29 − 2.58) 0.00062
BLCA 103 (25.50) 301 (74.50) 1.69 (1.15 − 2.49) 0.0074

◂**Fig. 2** IL1R2+Treg was positively associated with TNM Stage and poor prognosis in HNSCC. **A** Representative mIHC staining of CD4 (green), FOXP3 (red), IL1R2 (violet) and DAPI staining (gray) in human HNSCC tissues. Tregs (yellow) were identified using colocalization of CD4 and FOXP3. Scale bar, left, 20 μm; right, 5 μm. **B** Intensity of Treg (yellow) and IL1R2 (violet) was calculated using ImageJ according to the line on picture, related to Fig. 2A. **C** Representative mIHC staining of IL1R2+Treg in TMA ($n=69$) with different TNM stages. Scale bar, left, 20 μm; right, 10 μm. **D** Colocalization Intensity (below) of different TNM stages were calculated using ImageJ according to the lines on pictures above, related to Fig. 2C. **E** The proportion of IL1R2+Treg in Tregs was associated with TNM Stage, related to Fig. 2C. **F** Elisa analysis of serum soluble IL1R2 expression in HNSCC patients ($n=100$) and healthy donors ($n=40$). **G**, **H** Expression of serum soluble IL1R2 was related to metastasis (**G**) and TNM Stage (**H**). **I** Overall survival rate according to the proportion of IL1R2 in HNSCC tissues in a TCGA cohort. **J** HR according to IL1R2 in different cancer types in TCGA cohorts. HR, hazard ratio, THCA, Thyroid carcinoma, READ, Rectum adenocarcinoma, PDAC, Pancreatic ductal adenocarcinoma, LUAD, Lung adenocarcinoma, LIHC, Liver hepatocellular carcinoma, BLCA, Bladder carcinoma. sIL1R2, soluble IL1R2. ns, no significance; $^{*}p<0.05$; $^{**}p<0.01$; $^{***}p<0.001$; $^{****}p<0.0001$

termination solution was added to each well, and OD values were measured at 450 nm and 630 nm, respectively.

RNA interference

The siRNA for IL1R2 gene was designed and synthesized by Shanghai Genomeditech Company (Shanghai, China). The cells were transfected by using Lipofectamine 2000 (Thermo Fisher Scientific, USA) according to the manufacturer's instructions.

The siRNA sequence is as follows: IL-1R2-siRNA-1, 5′-CACAG GAAAG GUUUC UGAA tt-3′; IL-1R2-siRNA-2, 5′-CUCAA GGUCU UUAAG AAUA tt-3′; IL-1R2-siRNA-3, 5′-GGCUA UUACA GAUGU GUUA tt-3′.

C57BL/6 mice

MOC1 cells (5×10^5 cells/per site) were injected subcutaneously into the back of C57BL/6 mice. The tumor-bearing mice were divided into different groups: block-IL1R1 (400 ng per site), recombinant murine IL-1β (50 ng per site), si-IL1R2 (0.4 pmol per site), anti-CTLA4 (250 ng was injected intraperitoneally for each mice). Vernier calipers were used to measure tumor growth regularly. The calculation formula for tumor volume was $V=(L\times W^2)/2$, where V represented volume, L represented long diameter, and W represented short diameter.

Mass spectrometry

Tregs induced by naive CD4+T cells from the spleen of C57BL/6 mice, treated with IL-1β (50 ng/ml, TargetMol, #TMPY-02134). Tregs were then added CSK100 lysated cells (about 40 μl) containing PMSF (Phenylmethanesulfonyl fluoride). The supernatant containing cytoplasmic proteins was removed by centrifugation (4℃, 4000 rpm, 5 min). Cleaning precipitate with 200 μl CSK100 for three times (4℃, 4000 rpm, 5 min). The nuclear protein was collected by re-suspension precipitation with 25 μl whole cell lysate. Nuclear protein samples were subjected to Liquid Chromatography Mass Spectrometry by OE Biotech (Shanghai, China).

*CSK100 formula: 100 mM PIPES (pH = 6.8); 100 mM NaCl; 300 mM sucrose; 3 mM MgCl2; 1 mM EDTA; 0.5%TritonX-100; The rest is filled with ddH_2O.

Flow cytometry

Tumor samples were digested into single-cell suspension. Cells were incubated with LIVE/DEAD™ Fixable Violet Dead Cell Stain Kit (Invitrogen) for 30 min on ice and washed with PBS. Then a mix of fluorochrome-conjugated primary antibody (1:200, all purchased from Biolegend) was used, including PerCP/Cyanine5.5 anti-mouse CD45, FITC anti-mouse CD3ε, PE/Cyanine7 anti-mouse CD11b, Brilliant Violet 605 anti-mouse CD4, Brilliant Violet 510 anti-mouse CD8a, PE anti-mouse F4/80, APC anti-mouse CD206, PE anti-mouse CD279, PE/Cyanine7 anti-mouse CD152, Brilliant Violet 711 anti-mouse CD366, Brilliant Violet 605 anti-mouse CD279. For intracellular staining (Granzyme B, Perforin and IL1R2), cells were fixed and permeabilizated using BD Cytofix/Cytoperm™ Fixation/Permeabilization Kit (BD Pharmingen™). Then cells were stained with FITC anti-mouse Perforin (1:200, Biolegend), PE anti-mouse Granzyme B (1:200, Biolegend) and PE anti-mouse CD121b (1:100, BD Pharmingen™). For FOXP3 and NR4A1 staining, cells were stained with APC anti-mouse FOXP3 (1:100, eBioscience™) and PE anti-mouse NR4A1 (1:100, eBioscience™) after being fixed and permeabilizated using the Foxp3/Transcription Factor Staining Buffer Set (eBioscience™). The stained cells were resuspended in PBS, and NovoCyte Peatean (Agilent) was used to analyze single-cell suspension samples.

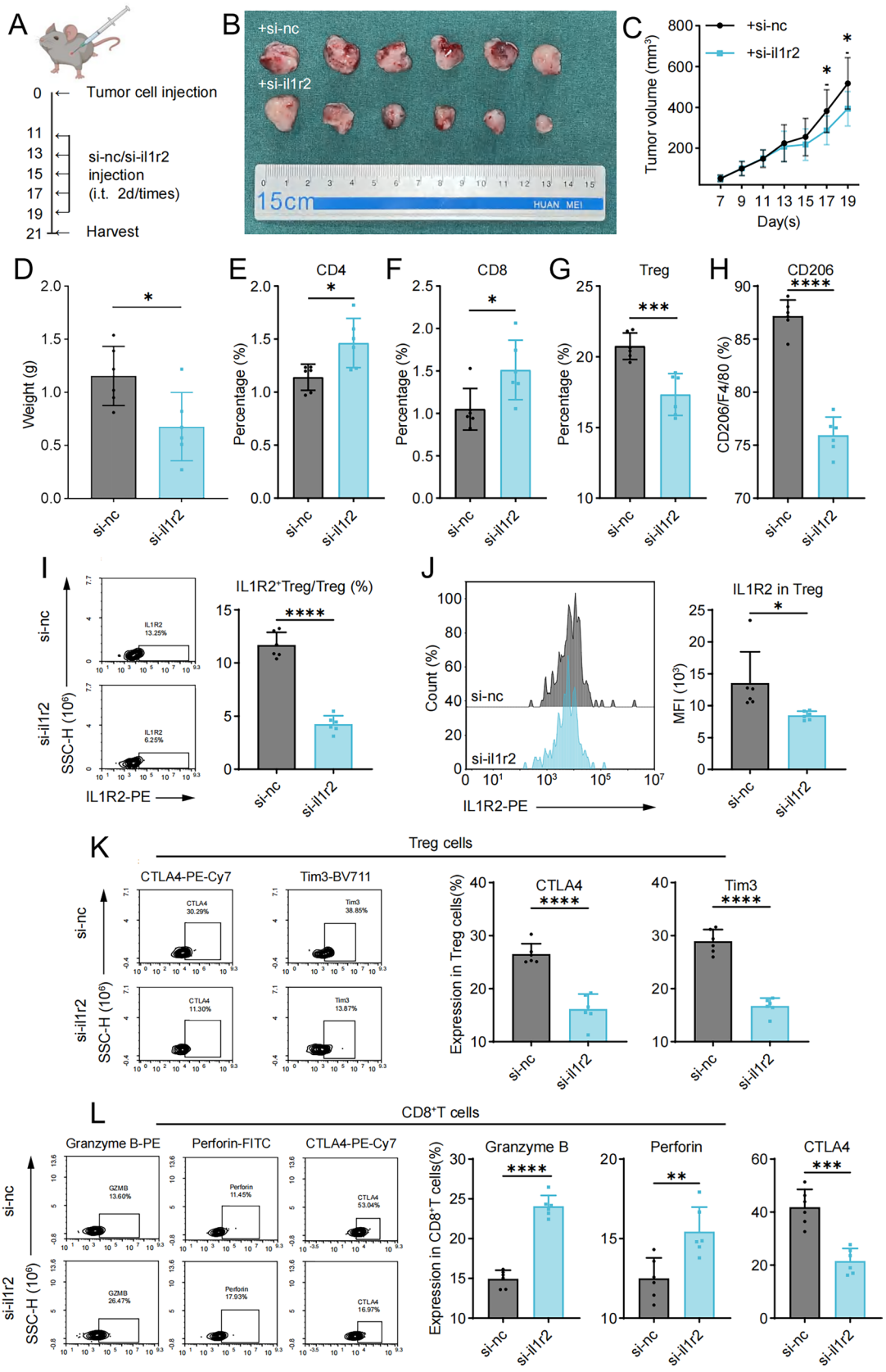
A
Tumor cell injection
si-nc/si-il1r2
injection
(i.t. 2d/times)
Harvest
B
+si-nc
+si-il1r2
15cm
C
+si-nc
+si-il1r2
Tumor volume (mm³)
Day(s)
D
Weight (g)
si-nc
si-il1r2
E
CD4
Percentage (%)
F
CD8
G
Treg
H
CD206
CD206/F4/80 (%)
I
IL1R2⁺Treg/Treg (%)
IL1R2-PE
SSC-H (10⁶)
J
IL1R2 in Treg
Count (%)
MFI (10³)
K
Treg cells
CTLA4-PE-Cy7
Tim3-BV711
Expression in Treg cells(%)
CTLA4
Tim3
L
CD8⁺T cells
Granzyme B-PE
Perforin-FITC
CTLA4-PE-Cy7
Expression in CD8⁺T cells(%)
Granzyme B
Perforin
CTLA4

◂**Fig. 3** Silencing IL1R2 inhibited tumor growth in vivo. **A** Schematic diagram showing the process for establishing the subcutaneous tumor models and treatments. **B** Images of isolated tumors. **C** Tumor growth after tumor cells injection and treatment. **D** Tumor weight after 21 days injection and treatment. **E**–**H** Average percentage of CD4+T cells (**E**), CD8+T cells (**F**), Treg cells (**G**) and M2 macrophages (CD206, **H**) in two groups identified by Flow Cytometry. Each group had 6 samples. **I**, **J** The proportion of IL1R2+Treg in Tregs (**I**) and the expression of IL1R2 in Treg (**J**). **K** Expression of CTLA4 and Tim3 in Tregs. **L** Expression of Granzyme B, Perforin and CTLA4 in CD8+T cells. i.t., intratumor injection. *$p<0.05$; **$p<0.01$; ***$p<0.001$; ****$p<0.0001$

Immunocytochemistry (ICC)

Tregs induced by naive CD4+T cells from mice spleen were seeded in coated confocal dishes. After stimulating with IL-1β (50 ng/ml, 12 h) with or without blocking IL1R2 for 24 h, the cells were then washed with pre-cooled PBS 2 times and fixed with 4% PFA for 15 min. TritonX-100 was used to permeabilize the cells, and 5% v/v goat serum in TBST was used for Fc blocking. The cells were incubated with primary antibodies at 4 °C overnight, washed with PBS 2 times and incubated with secondary antibodies for 1 h in the dark at room temperature. Nuclei were stained with DAPI for 15 min. Images of the cells were acquired with a Zeiss LSM900 microscope and further processed with ZEN 1.1.0.

RNA extraction and real-time PCR analysis

For cellular RNA extraction, Tregs were induced by naive CD4+T cells extracted from C57BL/6 mice spleen with murine IL-2 (10 ng/mL, Peprotech, #212–12) and TGF-β1 (10 ng/mL, Peprotech, #100–21) for 4 days after stimulating with α-CD3 (Biolegend, #100,238) and α-CD28 (Biolegend, #102,116). After different treatments, RNA was extracted with the RNA-Quick Purification Kit (ESunBio) according to the manufacturer's protocol. Reverse transcription was conducted with Evo M-MLV RT Master Mix (ACCURA TE BIOTECHNOLOGY(HUNAN)CO.,LTD, ChangSha, China, #AG11728). Hieff qPCR SYBR Green Master Mix (Yeasen) was used to conduct Real-time PCR. The $2^{-\Delta\Delta Ct}$ method was used to normalize the expression of target genes to that of Actb. The sequences used are as follows: Actb-F: GGCTGTATTCCCCTCCATCG, Actb-R: CCAGTTGGT AACAATGCCATGT; Il1r2-F: GCAGCAGATACGTGT GAGGAC, Il1r2-R: GTACCATGTCAGATTTACTGCCC; Ctla4-F: TTTTGTAGCCCTGCTCACTCT, Ctla4-R: CTG AAGGTTGGGTCACCTGTA.

Statistical analyses

Data shown in this study are means ± standard deviation (SD) of three independent experiments. A P value of <0.05 by using Student's t test was considered statistically significant.

Results

scRNA-seq identified the IL1R2+Treg subset in HNSCC

To analyze the infiltrating immune cells in the TME, we performed scRNA-seq on 5 pairs of HNSCC samples. Uniform manifold approximation and projection for dimension reduction (UMAP) were used to analyze different cell subsets in HNSCC. The results revealed that various cell types, such as epithelial cells, fibroblasts, Tregs and CD8+T cells, were present in HNSCC tumor tissues (Fig. 1A). The proportion of infiltrated Tregs, macrophages and CD8+T cells was increased significantly in tumor tissues compared to normal tissues (Fig. 1B). CD8+T cells were shown to exhibit an exhausted phenotype in our previous studies [13]. The proportion of Tregs increased from 4% in paracancerous tissue to 10% in tumor tissue (Fig. 1B), suggesting that Tregs may play an important role in the occurrence and development of HNSCC.

Tregs were further divided into 6 subsets (Fig. 1C). IL1R2+Treg was the most infiltrated Treg subset in tumor tissues (Fig. 1D). We analyzed the expression of markers of different Treg subsets in paired HNSCC samples and found that only the IL1R2 gene was significantly upregulated in tumor tissues (Fig. 1E, F). Subcellular localization analysis revealed that IL1R2 was predominantly expressed in Tregs (Fig. 1G; Supplementary Fig. S1A, B). Gene Ontology (GO) analysis revealed that the biological functions of the IL1R2+Treg include cytokine−cytokine receptor interactions, the regulation of immune cell activation, and the regulation of the CD8+T cell receptor (TCR) downstream signaling pathway (Fig. 1H). Moreover, we found that CTLA4 and HAVCR2 were upregulated in Tregs in tumor tissues compared to adjacent normal tissues (Fig. 1I). These results revealed a tumor-specific IL1R2+Treg in HNSCC, which might be related to immune response regulation.

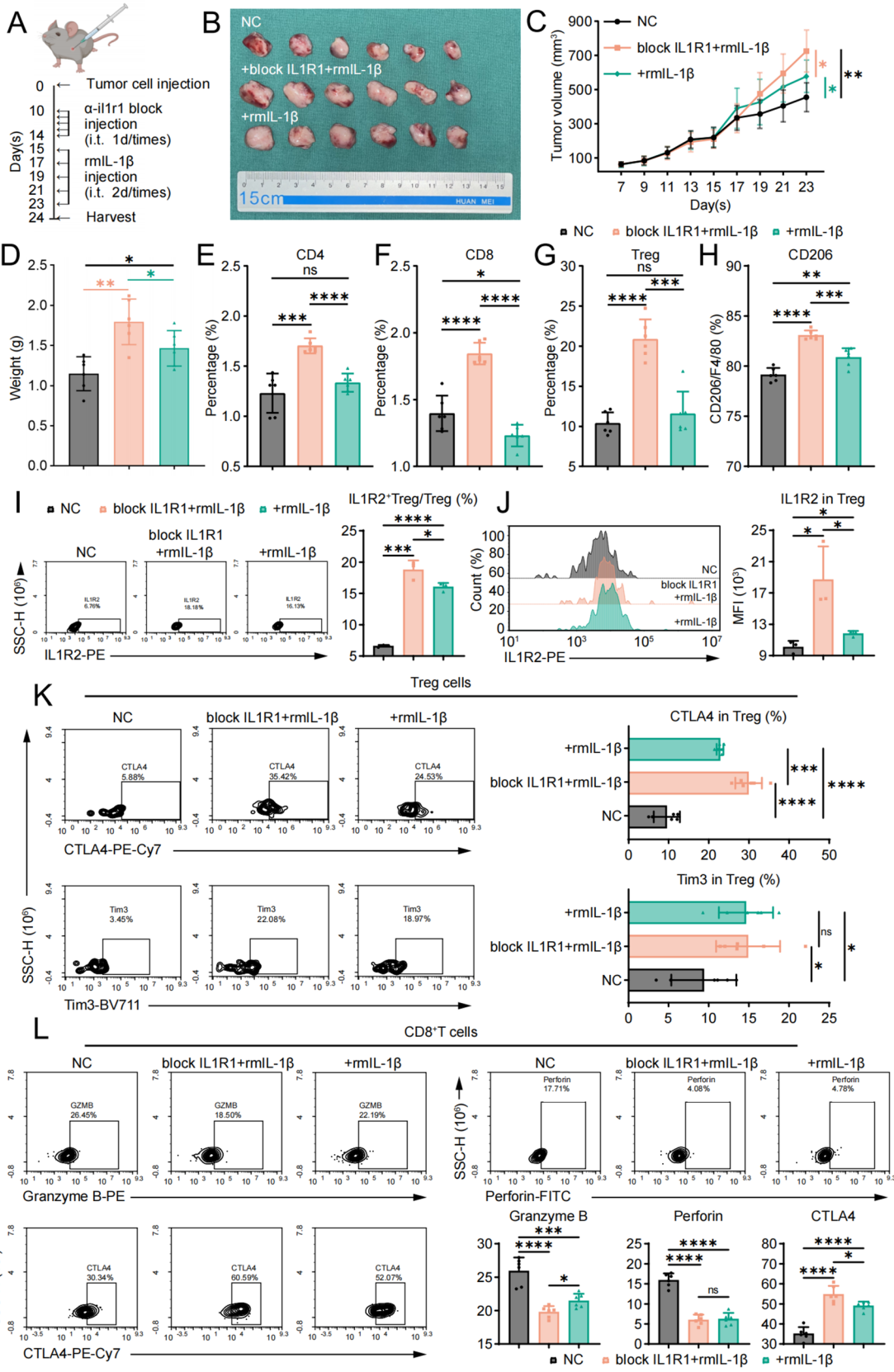
A
Tumor cell injection
α-il1r1 block injection (i.t. 1d/times)
rmIL-1β injection (i.t. 2d/times)
Harvest
Day(s)
B
NC
+block IL1R1+rmIL-1β
+rmIL-1β
15cm
C
NC
block IL1R1+rmIL-1β
+rmIL-1β
Tumor volume (mm³)
Day(s)
D
Weight (g)
E
CD4
Percentage (%)
F
CD8
G
Treg
H
CD206
CD206/F4/80 (%)
I
IL1R2⁺Treg/Treg (%)
SSC-H (10⁶)
IL1R2-PE
J
IL1R2 in Treg
Count (%)
MFI (10³)
K
Treg cells
CTLA4 in Treg (%)
CTLA4-PE-Cy7
Tim3 in Treg (%)
Tim3-BV711
L
CD8⁺T cells
Granzyme B-PE
Perforin-FITC
Granzyme B
Perforin
CTLA4

◂**Fig. 4** IL-1β promoted tumor growth and immunosuppressive TME formation. **A** Schematic diagram showing the process for establishing the subcutaneous tumor models and treatments. **B** Images of isolated tumors from 3 groups ($n=6$). **C** Tumor growth after tumor cells injection and treatment. **D** Tumor weight after 24 days injection and treatment. **E**–**H** Flow Cytometry showing the average percentage of CD4+T cells (**E**), CD8+T cells (**F**), Tregs (**G**) and M2 macrophages (CD206, **H**). **I**, **J** The proportion of IL1R2+Treg in Tregs (**I**) and the expression of IL1R2 in Treg (**J**). **K** Expression of CTLA4 and Tim3 in Tregs. **L** Expression and analysis of Granzyme B, Perforin and CTLA4 in CD8+T cells. i.t., intratumor injection. α-il1r1: anti-IL1R1. rmIL-1β: recombinant murine IL-1β. ns, no significance; $^{*}p<0.05$; $^{**}p<0.01$; $^{***}p<0.001$; $^{****}p<0.0001$

Diagnostic and prognostic value of the proportion of IL1R2+Treg in HNSCC

The levels of Treg markers (CD4 and FOXP3) and IL1R2 in clinical samples were assessed via multiplex immunohistochemistry (mIHC). The results proved that IL1R2+Treg did present in HNSCC samples (Fig. 2A, B). A TMA including 69 HNSCC samples revealed that the proportion of IL1R2+Treg was positively correlated with TNM stage but not with age, sex, tumor site, pathological grade or lymph node metastasis status in HNSCC patients (Fig. 2C–E). The diagnostic value of serum IL1R2 protein level was analyzed via ELISA of blood samples from 100 HNSCC patients and 40 healthy donors. The results revealed that the serum soluble IL1R2 level was significantly increased in HNSCC patients (Fig. 2F). What's more, the serum soluble IL1R2 level was positively correlated with HNSCC metastasis and TNM stage (Fig. 2G–H). These results indicated the importance of serum IL1R2 protein levels in the diagnosis of HNSCC. In addition, analysis of the cancer genome atlas (TCGA) database showed that a high proportion of IL1R2 was significantly associated with a poor HNSCC prognosis. HNSCC patients with greater infiltration of the IL1R2 had a worse prognosis (Fig. 2I). What's more, we also found that IL1R2+Treg was correlated with the response to anti-PD-1/CTLA-4 immunotherapy, which indicated that it had a predictive effect on the ICB treatment (Supplementary Fig. S1C). In addition to HNSCC, a high proportion of IL1R2 was significantly associated with a poor prognosis for rectum adenocarcinoma (READ), pancreatic ductal adenocarcinoma (PDAC), lung adenocarcinoma (LUAD), liver hepatocellular carcinoma (LIHC), and bladder urothelial carcinoma (BLCA) (Fig. 2J).

Silencing the IL1R2 gene inhibited tumor growth

An oral squamous cell carcinoma cell line (MOC1) was implanted subcutaneously into C57BL/6 mice to analyze the therapeutic value of IL1R2 in HNSCC (Fig. 3A). Compared with the control group, the tumor growth rate was lower, and the tumor volume and tumor weight were significantly lower in the si-il1r2 group (Fig. 3B–D). Further analysis revealed that the proportion of leukocytes and either lymphoid or myeloid cells was increased, whereas the proportion of M2 macrophages was significantly decreased (Fig. 3E–H; Supplementary Fig. S2A). After silencing the IL1R2 gene, the proportion of IL1R2+Treg and the expression of IL1R2, CTLA4 and Tim3 in Tregs decreased (Fig. 3I–K). Expression of Granzyme B and perforin in CD8+T cells was significantly increased, whereas CTLA4 expression was significantly decreased, which indicated the killing function of CD8+T cells was decreased while the exhaustion phenotype was upregulated (Fig. 3L; Supplementary Fig. S2A). The results showed that silencing the IL1R2 gene reduced the accumulation of IL1R2+Treg in tumors and reversed the immunosuppressive phenotype of the microenvironment in HNSCC.

IL-1β promoted the formation of an immunosuppressive microenvironment

IL1R2 has been reported to serve as a decoy receptor that competitively binds to IL-1β and prevents its binding to IL1R1 [5]. A recent study revealed that IL-1β was upregulated in many tumor tissues and our recent study indicated that IL-1β promoted tumor progression in HNSCC [14]. Thus, we analyzed the effect of IL-1β on HNSCC tumors in a tumor-bearing mouse model. Considering that IL1R1 also acts as a receptor for IL-1β, to demonstrate that the role of IL-1β in HNSCC tumors is mainly mediated by IL1R2, we used neutralizing antibodies to block the IL1R1 receptor in tumors and then injected recombinant murine IL-1β protein (rmIL-1β) (Fig. 4A). Compared with those in the negative control group, the tumor growth rate was greater in the rmIL-1β-treated group and the anti-IL1R1 + rmIL-1β-treated group, and the tumor volume and weight were significantly greater (Fig. 4B–D).

In the rmIL-1β-treated group and the anti-IL1R1 + rmIL-1β-treated group, the proportion of myeloid cells was increased, and the proportion of macrophages, especially M2 macrophages, was also increased (Fig. 4E–H; Supplementary Fig. S2B). Moreover, the proportion of IL1R2+Treg and the expression levels of IL1R2, CTLA4 and Tim3 in Tregs were significantly increased (Fig. 4I–K). Furthermore, in CD8+T cells, the levels of Granzyme B and perforin, which were cellular cytotoxicity markers, were significantly decreased, whereas the level of CTLA4 was significantly increased (Fig. 4L). The results showed that IL-1β significantly promoted the enrichment of IL1R2+Treg and the formation of an immunosuppressive microenvironment in HNSCC tumors.

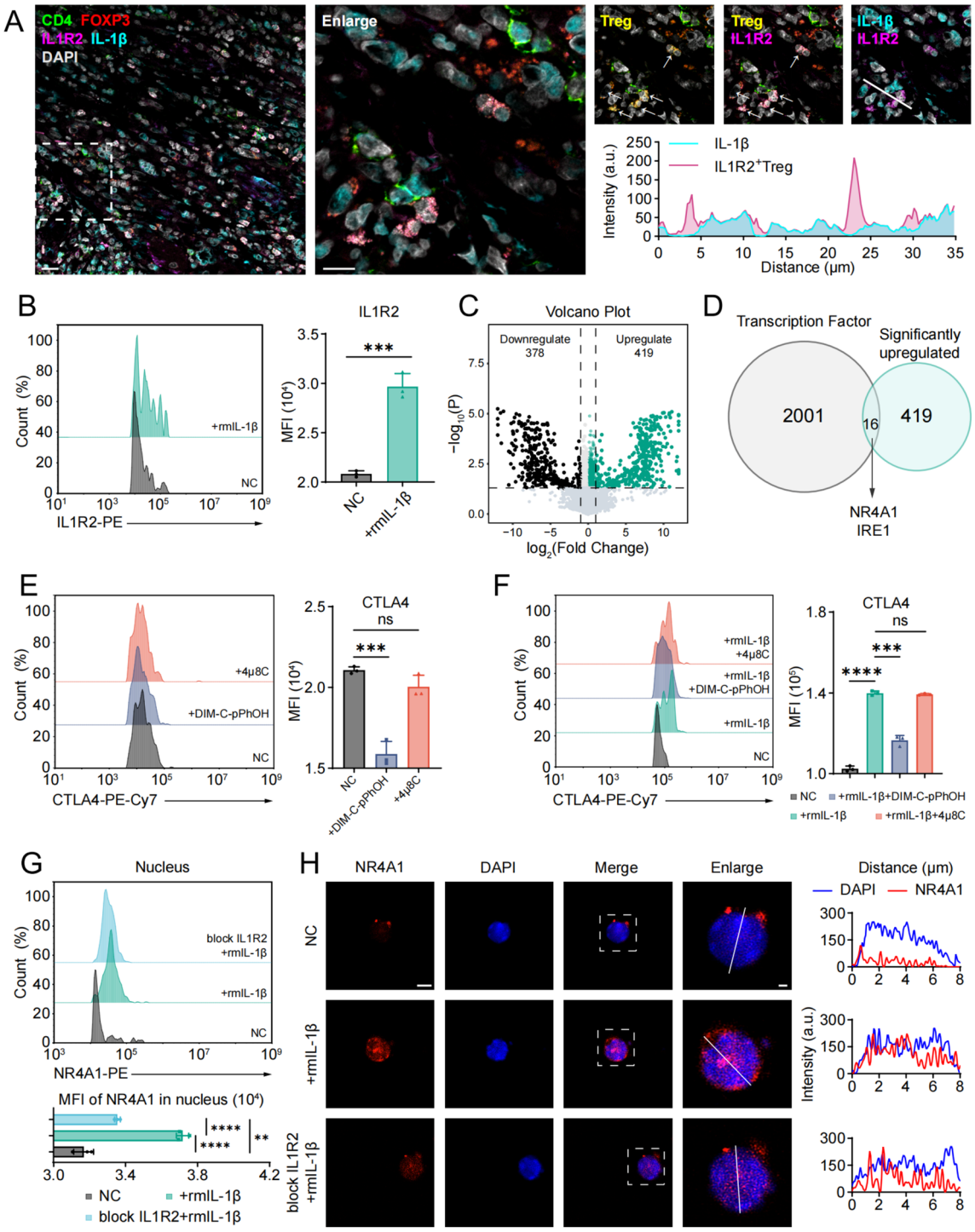

Fig. 5 IL-1β promoted the expression of the CTLA4 by regulating NR4A1. **A** Representative mIHC staining of CD4 (green), FOXP3 (red), IL1R2 (violet), IL-1β (cyan) in human HNSCC tissues. Tregs (yellow) were identified using colocalization of CD4 and FOXP3. Intensity of IL1R2+Treg (violet) and IL-1β (cyan) was calculated using ImageJ according to the line on picture. Scale bar, left, 20 μm; right, 10 μm. **B** Flow Cytometry showing the expression of IL1R2 in Tregs after treating with recombinant murine IL-1β for 12 h. **C** Volcano Plot showing significant down-regulated and up-regulated nuclear protein after treating with rmIL-1β (50 ng/mL) measured by Pro DIA quantitative proteomics. **D** Venn diagram showed 16 genes both up-regulated significantly in rmIL-1β group and worked as transcription factor. **E**, **F** The expression of CTLA4 in Tregs after using DIM-C-pPhOH (NR4A1 inhibitor, 20 μM, 24 h) and 4μ8C (IRE1 inhibitor, 200 nM, 24 h) with (F) or without (E) treating with rmIL-1β. **G** The expression of NR4A1 in nucleus in Tregs after stimulating with rmIL-1β or blocking IL1R2. **H** The location and intensity of NR4A1 in Tregs with different treatments. Scale bar, left, 2 μm; right, 1 μm. Intensity of NR4A1 (red) and DAPI (blue) was calculated using ImageJ according to the line on picture. ns, no significance; *$p < 0.05$; **$p < 0.01$; ***$p < 0.001$; ****$p < 0.0001$

IL-1β promoted the expression of CTLA4 in Tregs by regulating NR4A1

Next, mIHC analysis revealed that IL-1β and IL1R2+Treg colocalized in the HNSCC TME, suggesting that IL-1β might be a ligand for IL1R2+Treg (Fig. 5A). On the basis of our in vivo results, we explored how IL-1β affected Tregs in vitro. After stimulating Tregs with rmIL-1β for 12 h, we found that the expression of IL1R2 was upregulated (Fig. 5B). These results were consistent with our previous scRNA-seq results (Fig. 1I). To further explore how IL-1β regulated CTLA4 in IL1R2+Treg, we separated nuclear proteins from Tregs with or without IL-1β stimulation and analyzed them via protein spectrometry. Selecting transcription factors which were significantly upregulated in Tregs' nucleus, we identified NR4A1 and IRE1 as candidate transcription factors (Fig. 5C, D; Supplementary Table. S1). Using DIM-C-pPhOH (NR4A1 inhibitor, 20 μM) [15] and 4μ8C (IRE1 inhibitor, 200 nM) [16], we found that inhibiting NR4A1 reduced the expression of CTLA4 even stimulated with rmIL-1β, thus we hypothesized that IL-1β regulated CTLA4 via NR4A1 (Fig. 5E, F). After using rmIL-1β and blocking IL1R2, we verified that IL-1β translocated NR4A1 into nucleus to promote CTLA4 transcription (Fig. 5G, H). Besides, we wondered if NR4A1 regulated the expression of IL1R2 in Tregs, after using DIM-C-pPhOH (20 μM) for a 24 h-blocking, we found that NR4A1 did not upregulated IL1R2 but only CTLA4 at both protein and mRNA level (Supplementary Fig. S3A–D).

Combined targeting of IL1R2 and CTLA4 to inhibit tumor growth

In vivo experiments were used to explore whether silencing IL1R2 alone or neutralizing CTLA4 alone could inhibit tumor growth and whether combined targeting of IL1R2 and CTLA4 had a more significant inhibitory effect on tumor growth (Fig. 6A–D). We also found that the TME changed, and the proportion of M2 macrophages decreased after treatment with either alone or combined (Fig. 6E–H; Supplementary Fig. SC). Combined targeting of IL1R2 and CTLA4 had the most significant inhibitory effect on IL1R2 gene expression in Tregs and decreased the expression of CTLA4 and Tim3 in Tregs (Fig. 6I–K). The combination of si-il1r2 and anti-CTLA4 promoted the killing function of CD8+T cells and inhibited the expression of CTLA4 in CD8+T cells (Fig. 6L). Taken together, these results indicated that combined targeting of IL1R2 and CTLA4 was an effective strategy to inhibit tumor growth and regulate the immunosuppressive TME (Fig. 7).

Discussion

Some studies have revealed that there are different Treg subsets that respond to different signals, such as IFNα-responsive Tregs and TNFR-responsive Tregs [17]. Also, the collagen-induced LAIR2 + Treg subset was reported to promoted the formation of a TME which was favorable for tumor progression [18]. However, there are few studies on Treg subsets in HNSCC. In this study, we found that the IL1R2+Treg highly infiltrated HNSCC tumor tissues and was positively associated with advanced TNM stage and a poor prognosis in HNSCC. Moreover, the expression of soluble IL1R2 level in serum was positively correlated with tumor metastasis and the TNM stage of HNSCC. In addition to HNSCC, IL1R2+Treg was also found to exhibit enrichment in esophageal cancer and in colorectal adenoma [19]. Using TCGA database, we also explored that IL1R2+Treg had a predictive effect on the ICB treatment and IL1R2 was related to a poor prognosis in READ, PDAC, LUAD, LIHC and BLCA. These results indicate that IL1R2+Treg may play a broad role in immune escape and may be valuable for tumor diagnosis.

IL1R2 plays an important role in tumorigenesis, angiogenesis, invasion and metastasis through immune regulation, and has a potential carcinogenic effect. The upregulation of IL1R2 has been observed in various cancers, such as colorectal cancer [11], gastric cancer [20], breast cancer [21], lung cancer [22], PDAC [23], prostate cancer [24], ovarian cancer [25], and oral cancer [26]. Silencing IL1R2 expression inhibited the proliferation of osteosarcoma cells [27]. What's more, blocking IL1R2 expression can reduce the enrichment of breast cancer stem cells in tumor tissues, inhibit the infiltration of tumor-associated macrophages, and reverse the exhausted phenotype of CD8+T cells [28]. In this study, we found that silencing the IL1R2 gene significantly suppressed the infiltration of the IL1R2+Treg and M2 macrophages in the TME, enhanced the killing activity of CD8+T cells, and inhibited tumor growth. These results indicated that IL1R2 was not only a potential diagnostic biomarker but also a potential new treatment target for HNSCC.

Interleukin-1β (IL-1β) is a pro-inflammatory mediator that can bind with IL1R2. Recent studies found that the expression of IL-1β was elevated in tumors and either IL-1β or IL-1β + TAMs promoted tumor progression, such as HNSCC and PDAC [14, 29]. This study confirmed that IL-1β colocalized with IL1R2+Treg in HNSCC tumor samples, and IL-1β significantly upregulated the expression of IL1R2 in Tregs, promoting the formation of an immunosuppressive TME. These results indicated that IL-1β was an important factor that promoted IL1R2+Treg formation and enrichment in tumors.

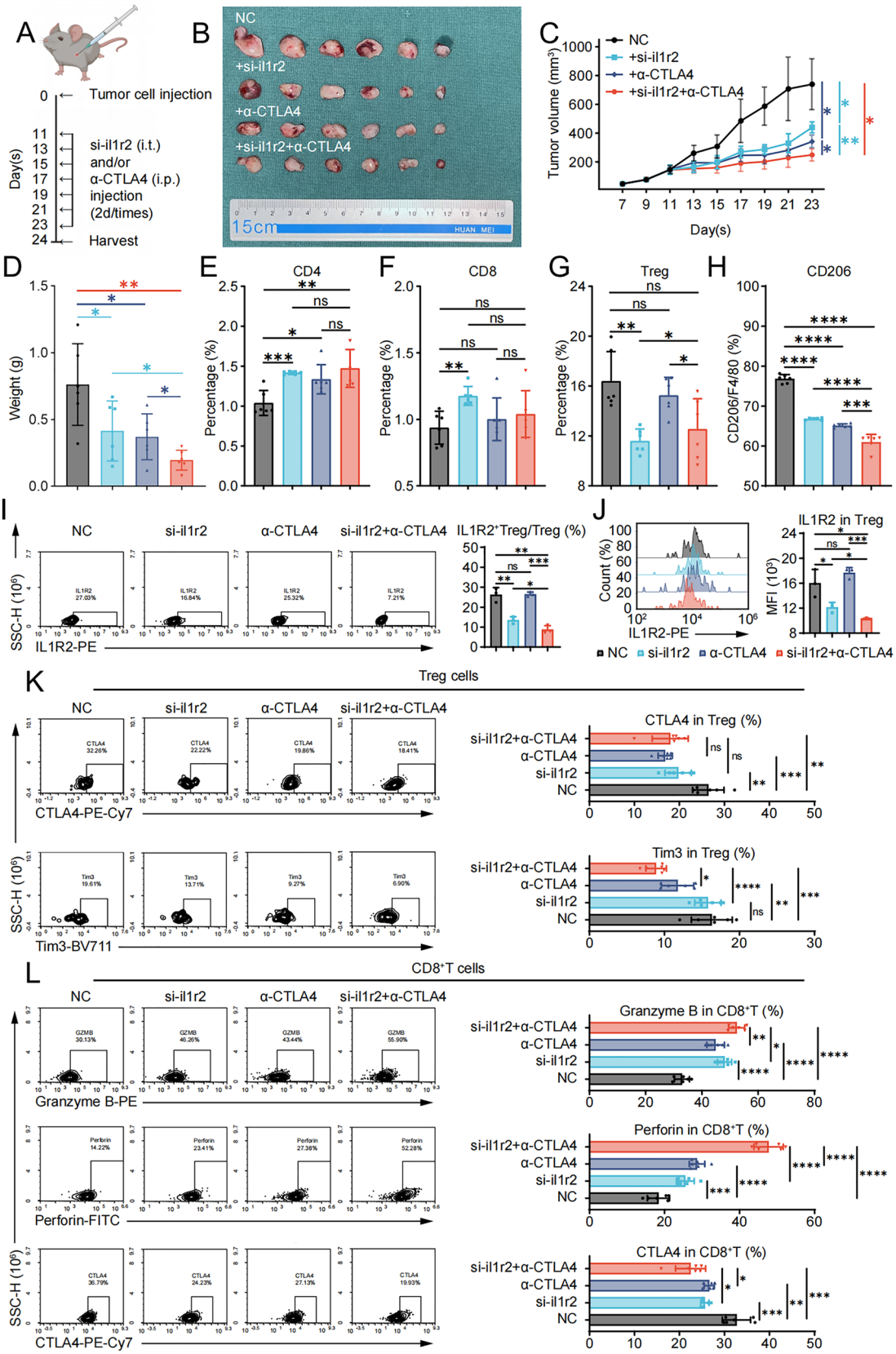
A
Tumor cell injection
si-il1r2 (i.t.)
and/or
α-CTLA4 (i.p.)
injection
(2d/times)
Harvest
Day(s)
B
NC
+si-il1r2
+α-CTLA4
+si-il1r2+α-CTLA4
15cm
C
NC
+si-il1r2
+α-CTLA4
+si-il1r2+α-CTLA4
Tumor volume (mm³)
Day(s)
D
Weight (g)
E
CD4
Percentage (%)
F
CD8
Percentage (%)
G
Treg
Percentage (%)
H
CD206
CD206/F4/80 (%)
I
NC
si-il1r2
α-CTLA4
si-il1r2+α-CTLA4
SSC-H (10⁶)
IL1R2-PE
IL1R2⁺Treg/Treg (%)
J
Count (%)
IL1R2-PE
IL1R2 in Treg
MFI (10³)
K
Treg cells
CTLA4-PE-Cy7
CTLA4 in Treg (%)
Tim3-BV711
Tim3 in Treg (%)
L
CD8⁺T cells
Granzyme B-PE
Granzyme B in CD8⁺T (%)
Perforin-FITC
Perforin in CD8⁺T (%)
CTLA4-PE-Cy7
CTLA4 in CD8⁺T (%)

◂**Fig. 6** Combined targeting of IL1R2 and CTLA4 inhibited tumor growth and immunosuppressive microenvironment formation. **A** Schematic diagram showing the process for establishing the subcutaneous tumor models and treatments. **B** Images of isolated tumors from 4 groups ($n=6$). **C** Tumor growth after tumor cells injection and treatment. **D** Tumor weight after 24 days injection and treatment. **E**–**H** Flow Cytometry showing the average percentage of CD4+T cells (**E**), CD8+T cells (**F**), Tregs (**G**) and M2 macrophages (CD206, **H**). **I**, **J** The proportion of IL1R2+Treg in Tregs (**I**) and the expression of IL1R2 in Treg (**J**). **K** Expression of CTLA4 and Tim3 in Tregs. **L** Expression and analysis of Granzyme B, Perforin and CTLA4 in CD8+T cells. i.t., intratumor injection. i.p., intraperitoneal injection. α-CTLA4, anti-CTLA4 antibody. ns, no significance; *$p<0.05$; **$p<0.01$; ***$p<0.001$; ****$p<0.0001$

As a key molecule that mediates the immunosuppressive activity of Tregs, the expression level of CTLA4 is regulated by many factors. The Nuclear factor of activated T-cells (NFAT) can promote the expression of the CTLA4 gene [30]. CTLA4 can also be epigenetically regulated by promoter DNA methylation, and its transcriptional activity is related to the DNA methylation status of the promoter region [31]. In addition, lactic acid can promote the RNA splicing of CTLA4 in Tregs and maintain the immunosuppressive function of Tregs [32]. In this study, we found that IL-1β promoted the expression of IL1R2 and further regulated transcription factor NR4A1. NR4A1, also known as Nur77, is a member of the superfamily of orphan nuclear receptors. It has been reported that NR4A1 was important in Treg cells maintenance [33]. Another studies indicated that NR4A1 promoted cancer cells metastasis through enhancing immunosuppressive function of Tregs [34]. A recent studies also showed that, in CD8+T cells, NR4A1 promoted Tpex development and the expression of Tox and TCF7 during tumorigenesis and chronic virus infection [35]. Here, we also found that IL-1β translocated NR4A1 into nucleus and thus upregulated the expression of CTLA4, but not regulated IL1R2, which providing a new understanding of the transcriptional regulation of CTLA4 in Tregs.

Ipilimumab has shown promise in a variety of malignancies, but there are still many challenges in the application of ipilimumab as a single agent, such as the high incidence and grade of adverse events associated with anti-CTLA4 therapy. Considering the above disadvantages, ipilimumab is often used in combination with other drugs, such as the indoleamine 2,3-dioxygenase inhibitor INCB024360 and granulocyte−macrophage colony−stimulating factor [36, 37]. The results of this study indicated that the combined blockade of IL1R2 and CTLA4 might be an effective anti-HNSCC strategy. Compared with the monotherapy group, the combined treatment group had more significant antitumor effects. What's more, we found that using anti-CTLA4 alone might upregulated the expression of PD-1 in both CD8+T cells and Tregs. It may due to using anti-CTLA4 changed the TME and promoted the expression of PD-1 by activating genes related [38, 39]. However, when using si-il1r2 combined, PD-1 level in CD8+T cells and Tregs was downregulated significantly, which also showed an antitumor effect.

In conclusion, we found that IL-1β promoted the expression of IL1R2 in Tregs and further promoted CTLA4 expression in Tregs by inducing the nuclear translocation

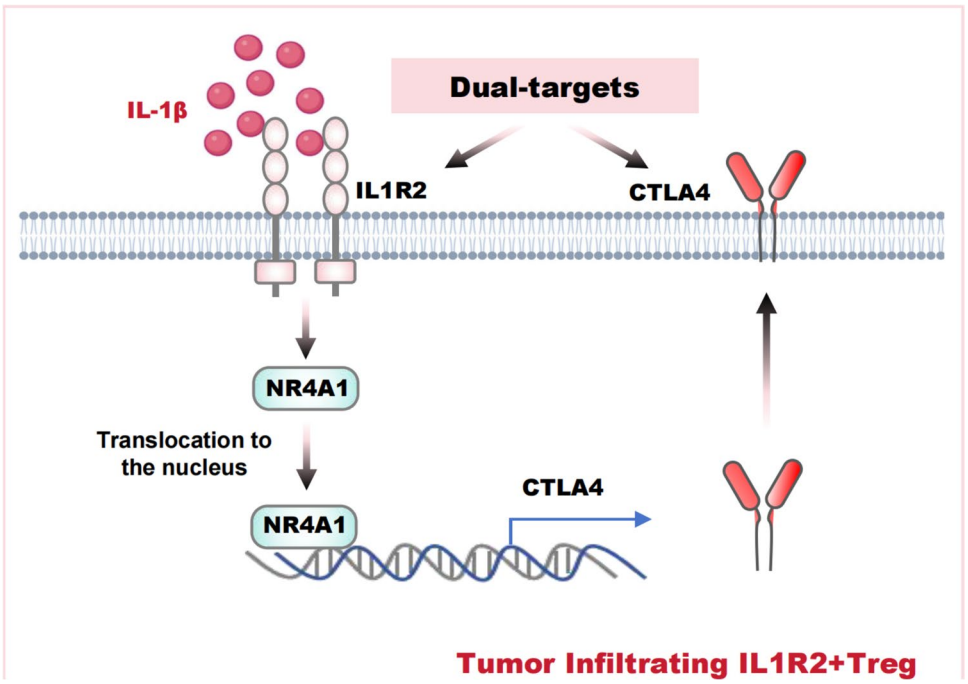

Fig. 7 The proposed model for this study

of NR4A1. Combined targeting of IL1R2 and CTLA4 may be a promising strategy to inhibit HNSCC progression.

Supplementary Information The online version contains supplementary material available at https://doi.org/10.1007/s00262-025-04015-1.

Author contributions H.G. designed and performed experiments, analyzed the data and wrote the manuscript; C. L. performed experiments, analyzed the data and contributed to methodology; K. W. performed formal analysis and wrote the manuscript; Y. L. analyzed the data and contributed to methodology; Z. Z. and F. C. revised the manuscript and supervised all parts of project. All authors read and approved the final manuscript. All authours reviewed and approved the manuscript.

Funding This study was supported by grants from the Project of National Natural Science Foundation of China (grant no. 82273267), Fundamental research program funding of Ninth People's Hospital affiliated to Shanghai Jiao Tong university School of Medicine (JYZZ180).

Data availability The single-cell transcriptomics data used in this study are publicly available in the Genome Sequence Archive (https://ngdc.cncb.ac.cn/gsa-human/browse/HRA005576) and nonprofit research will be approved for access for these data.

Declarations

Conflict of interest The authors declare that they have no conflict of interest.

Ethical approval The Ethics Committee of the Ninth People's Hospital, Shanghai Jiao Tong University School of Medicine, approved this study. Written informed consent was obtained from all participants before starting the experiment. All experimental methods abided by the Declaration of Helsinki. All animal experiments were approved by the Animal Care and Use Committee of the Ninth People's Hospital, Shanghai Jiao Tong University School of Medicine. Registry and the Registration No. of the study/trial: No. SH9H-2024-TK69-1. Animal Studies: No.SH9H-2024-A054-SB.

References

1. Shan F, Somasundaram A, Bruno TC, Workman CJ, Vignali DAA (2022) Therapeutic targeting of regulatory T cells in cancer. Trends Cancer 8:944–961
2. Dadey RE, Workman CJ, Vignali DAA (2020) Regulatory T cells in the tumor microenvironment. Adv Exp Med Biol 1273:105–134
3. Sawant DV, Yano H, Chikina M, Zhang Q, Liao M, Liu C et al (2019) Adaptive plasticity of IL-10(+) and IL-35(+) T(reg) cells cooperatively promotes tumor T cell exhaustion. Nat Immunol 20:724–735
4. Jie HB, Gildener-Leapman N, Li J, Srivastava RM, Gibson SP, Whiteside TL et al (2013) Intratumoral regulatory T cells upregulate immunosuppressive molecules in head and neck cancer patients. Br J Cancer 109:2629–2635
5. Peters VA, Joesting JJ, Freund GG (2013) IL-1 receptor 2 (IL-1R2) and its role in immune regulation. Brain Behav Immun 32:1–8
6. Supino D, Minute L, Mariancini A, Riva F, Magrini E, Garlanda C (2022) Negative regulation of the IL-1 system by IL-1R2 and IL-1R8: relevance in pathophysiology and disease. Front Immunol 13:804641
7. Molgora M, Supino D, Mantovani A, Garlanda C (2018) Tuning inflammation and immunity by the negative regulators IL-1R2 and IL-1R8. Immunol Rev 281:233–247
8. Colotta F, Saccani S, Giri JG, Dower SK, Sims JE, Introna M et al (1996) Regulated expression and release of the IL-1 decoy receptor in human mononuclear phagocytes. J Immunol 156:2534–2541
9. Mantovani A, Barajon I, Garlanda C (2018) IL-1 and IL-1 regulatory pathways in cancer progression and therapy. Immunol Rev 281:57–61
10. Voronov E, Apte RN (2017) Targeting the tumor microenvironment by intervention in interleukin-1 biology. Curr Pharm Des 23:4893–4905
11. Mar AC, Chu CH, Lee HJ, Chien CW, Cheng JJ, Yang SH et al (2015) Interleukin-1 receptor type 2 acts with c-Fos to enhance the expression of interleukin-6 and vascular endothelial growth factor A in colon cancer cells and induce angiogenesis. J Biol Chem 290:22212–22224
12. Liu Y, Xing Z, Yuan M, Xu B, Chen L, Zhang D et al (2022) IL1R2 promotes tumor progression via JAK2/STAT3 pathway in human clear cell renal cell carcinoma. Pathol Res Pract 238:154069
13. Li C, Guo H, Zhai P, Yan M, Liu C, Wang X et al (2024) Spatial and single-cell transcriptomics reveal a cancer-associated fibroblast subset in HNSCC that restricts infiltration and antitumor activity of CD8+T cells. Cancer Res 84:258–275
14. Liu C, Wu K, Li C, Zhang Z, Zhai P, Guo H et al (2024) SPP1+ macrophages promote head and neck squamous cell carcinoma progression by secreting TNF-α and IL-1β. J Exp Clin Cancer Res 43(1):332
15. Hedrick E, Lee SO, Kim G, Abdelrahim M, Jin UH, Safe S et al (2015) Nuclear receptor 4A1 (NR4A1) as a drug target for renal cell adenocarcinoma. PLoS ONE 10(6):e0128308
16. Ranatunga S, Tang CH, Kang CW, Kriss CL, Kloppenburg BJ, Hu CCA et al (2014) Synthesis of novel tricyclic chromenone-based inhibitors of IRE-1 RNase activity. J Med Chem 57(10):4289–4301
17. Cillo AR, Kurten CHL, Tabib T, Qi Z, Onkar S, Wang T et al (2020) Immune landscape of viral- and carcinogen-driven head and neck cancer. Immunity 52:183-199e9
18. Choi JH, Lee BS, Jang JY, Lee YS, Kim HJ, Roh J et al (2023) Single-cell transcriptome profiling of the stepwise progression of head and neck cancer. Nat Commun 14:1055
19. Zheng Y, Chen Z, Han Y, Han L, Zou X, Zhou B et al (2020) Immune suppressive landscape in the human esophageal squamous cell carcinoma microenvironment. Nat Commun 11:6268
20. Yuan M, Wang L, Huang H, Li Y, Zheng X, Shao Q et al (2021) IL-1R2 expression in human gastric cancer and its clinical significance. Biosci Rep 41:BSR20204425

21. Zhang L, Qiang J, Yang X, Wang D, Rehman AU, He X et al (2020) IL1R2 blockade suppresses breast tumorigenesis and progression by impairing USP15-dependent BMI1 stability. Adv Sci (Weinh) 7:1901728
22. Wang C, Zhang C, Xu J, Li Y, Wang J, Liu H et al (2019) Association between IL-1R2 polymorphisms and lung cancer risk in the Chinese Han population: a case-control study. Mol Genet Genom Med 7:e644
23. Herremans KM, Szymkiewicz DD, Riner AN, Bohan RP, Tushoski GW, Davidson AM et al (2022) The interleukin-1 axis and the tumor immune microenvironment in pancreatic ductal adenocarcinoma. Neoplasia 28:100789
24. Miaskowski C, Cataldo JK, Baggott CR, West C, Dunn LB, Dhruva A et al (2015) Cytokine gene variations associated with trait and state anxiety in oncology patients and their family caregivers. Support Care Cancer 23(4):953–965
25. Fattahi A, Zarezadeh R, Rastgar Rezaei Y, Mettler L, Nouri M, Schmutzler AG et al (2023) Expression of interleukin-1β and its receptor in human granulosa cells and their association with steroidogenesis. Tissue Cell 85:102230
26. Liu S, Zhou X, Peng X, Li M, Ren B, Cheng G et al (2020) *Porphyromonas gingivalis* promotes immunoevasion of oral cancer by protecting cancer from macrophage attack. J Immunol 205:282–289
27. Liu X, Min L, Duan H, Shi R, Zhang W, Hong S et al (2018) Expression of concern: short hairpin RNA (shRNA) of type 2 interleukin-1 receptor (IL1R2) inhibits the proliferation of human osteosarcoma U-2 OS cells. Med Oncol 35(10):129
28. Xia J, Zhang L, Peng X, Tu J, Li S, He X et al (2024) IL1R2 blockade alleviates immunosuppression and potentiates anti-PD-1 efficacy in triple-negative breast cancer. Cancer Res 84:2282–2296
29. Yang D, Sun X, Wang H, Wistuba II, Wang H, Maitra A et al (2025) TREM2 depletion in pancreatic cancer elicits pathogenic inflammation and accelerates tumor progression via enriching IL-1β+ macrophages. Gastroenterology S0016–5085(25):00368–00373
30. Gibson HM, Hedgcock CJ, Aufiero BM, Wilson AJ, Hafner MS, Tsokos GC et al (2007) Induction of the CTLA-4 gene in human lymphocytes is dependent on NFAT binding the proximal promoter. J Immunol 179:3831–3840
31. Klumper N, Ralser DJ, Zarbl R, Schlack K, Schrader AJ, Rehlinghaus M et al (2021) CTLA4 promoter hypomethylation is a negative prognostic biomarker at initial diagnosis but predicts response and favorable outcome to anti-PD-1 based immunotherapy in clear cell renal cell carcinoma. J Immunother Cancer 9:e002949
32. Ding R, Yu X, Hu Z, Dong Y, Huang H, Zhang Y et al (2024) Lactate modulates RNA splicing to promote CTLA-4 expression in tumor-infiltrating regulatory T cells. Immunity 57:528-540e6
33. Gao L, Wang H, Fang F, Liu J, Zhao C, Niu J et al (2024) The roles of orphan nuclear receptor 4 group A1 and A2 in fibrosis. Int Immunopharmacol 139:112705
34. Carelock ME, Master RP, Kim MC, Jin Z, Wang L, Maharjan CK et al (2023) Targeting intracellular proteins with cell type-specific functions for cancer immunotherapy. Life Med 2(3):lnad019
35. Hao J, Li R, Zhao X, Liu X, Chen X, Xie T et al (2024) NR4A1 transcriptionally regulates the differentiation of stem-like CD8+ T cells in the tumor microenvironment. Cell Rep 43(6):114301
36. Beatty GL, O'Dwyer PJ, Clark J, Shi JG, Bowman KJ, Scherle PA et al (2017) First-in-human phase i study of the oral inhibitor of indoleamine 2,3-dioxygenase-1 epacadostat (INCB024360) in patients with advanced solid malignancies. Clin Cancer Res 23:3269–3276
37. Chesney J, Puzanov I, Collichio F, Singh P, Milhem MM, Glaspy J et al (2018) Randomized, open-label phase II study evaluating the efficacy and safety of talimogene laherparepvec in combination with ipilimumab versus ipilimumab alone in patients with advanced, unresectable melanoma. J Clin Oncol 36:1658–1667
38. Campbell KM, Amouzgar M, Pfeiffer SM, Howes TR, Medina E, Travers M et al (2023) Prior anti-CTLA-4 therapy impacts molecular characteristics associated with anti-PD-1 response in advanced melanoma. Cancer Cell 41(4):791-806.e4
39. Willsmore ZN, Coumbe BGT, Crescioli S, Reci S, Gupta A, Harris RJ et al (2021) Combined anti-PD-1 and anti-CTLA-4 checkpoint blockade: treatment of melanoma and immune mechanisms of action. Eur J Immunol 51(3):544–556